Expanded View Figures

A RNA-seq data *Rpp30*$^{18.2}$/*white* virgin ovaries:

Gene identity	log2foldChange	pValue
FBgn0022246 (Rpp30)	−1.163357556	0.000508915

B Germline clones *Rpp30*$^{18.2}$

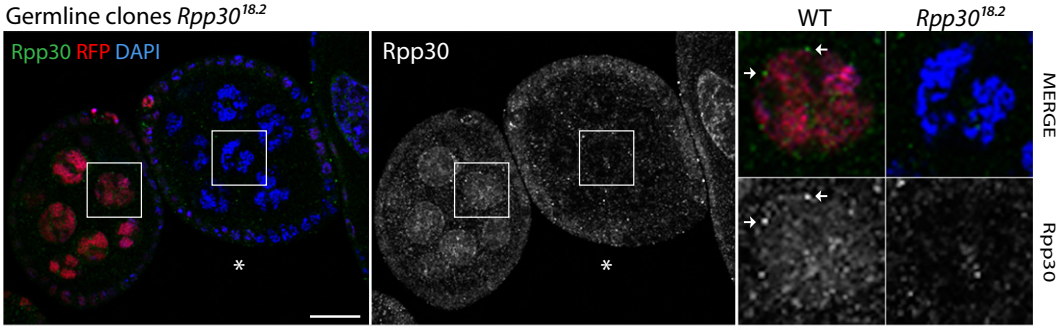

C Somatic clones *Rpp30*$^{18.2}$

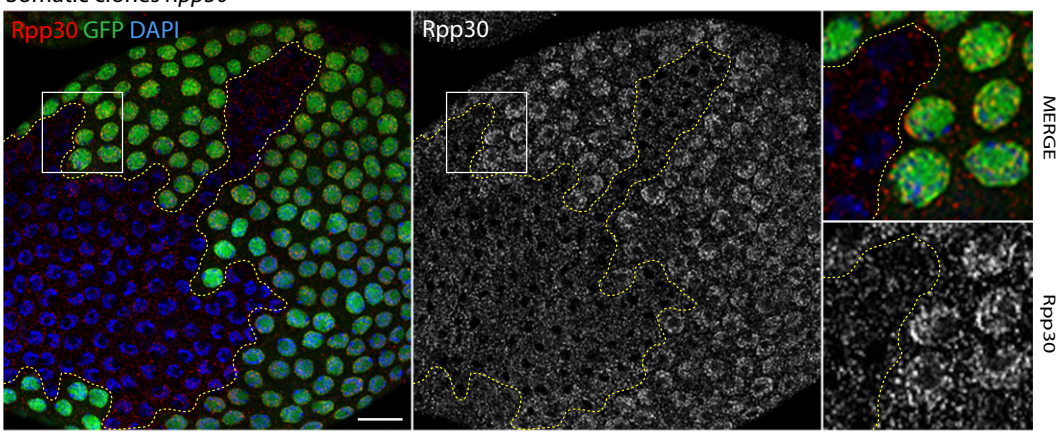

D *Rpp30*$^{18.2}$*; ubiRpp30GFP*

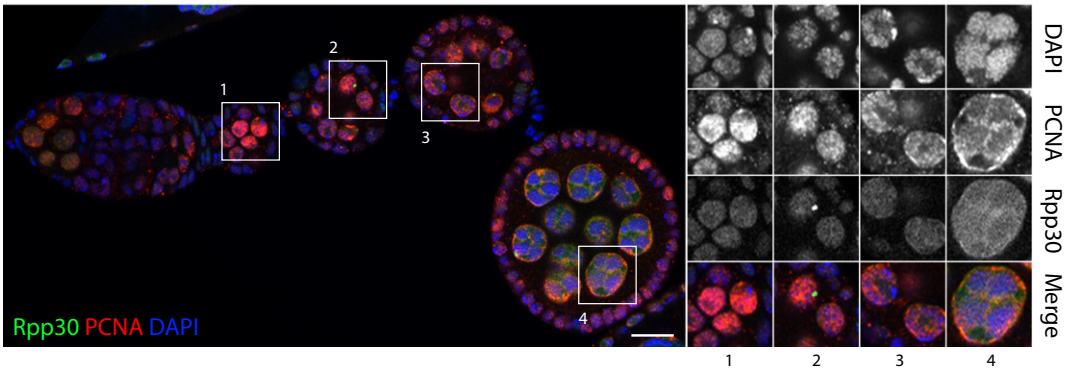

Figure EV1. Rpp30 protein expression is affected in *Rpp30*$^{18.2}$ mutants and PCNA loss in *Rpp30*$^{18.2}$ ovaries is restored when overexpressing *ubiRpp30GFP* (related to Figs 1 and 3).

A Normalized fold change and *P*-value between *Rpp30*$^{18.2}$ mutant ovaries and *white* virgins issue from RNA-seq transcriptome analysis showing a downregulation of *Rpp30* transcripts in *Rpp30*$^{18.2}$ mutant ovaries.

B, C flp/FRT clones mutant for *Rpp30*$^{18.2}$ specifically in the germ line (B) or follicular cells (C) are detected by the absence of RFP or GFP, respectively. Magnifications show Rpp30 absence in the nucleus of mutant cells. Perinuclear Rpp30 foci are indicated by white arrows in a wild-type nurse cell (B). Scale bar, 10 μm.

D *Rpp30*$^{18.2}$ homozygous ovaries overexpressing *ubiRpp30GFP* were dissected, fixed, and stained for PCNA (red). Rpp30GFP is in green and DAPI is in blue. Scale bar, 10 μm.

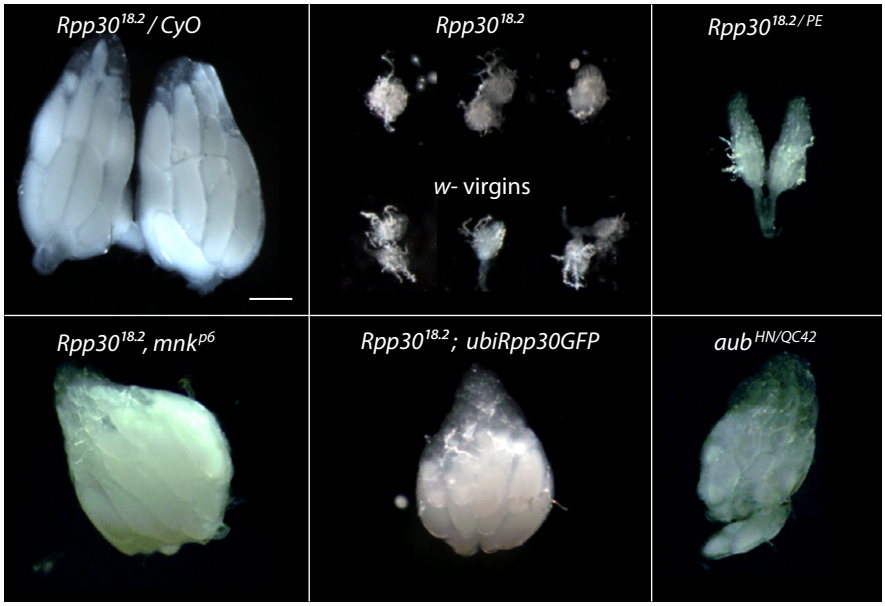

Figure EV2. Size of ovaries used in this work (related to Figs 4–6).
Ovaries of different genotypes used for small RNA sequencing, RNA sequencing, and ChIP analysis. The left panel of heterozygous *Rpp30$^{18.2}$/CyO* ovaries has been included again in this figure (also present in Fig 1A) in order to better compare the different ovaries used altogether. Scale bar, 100 μm.

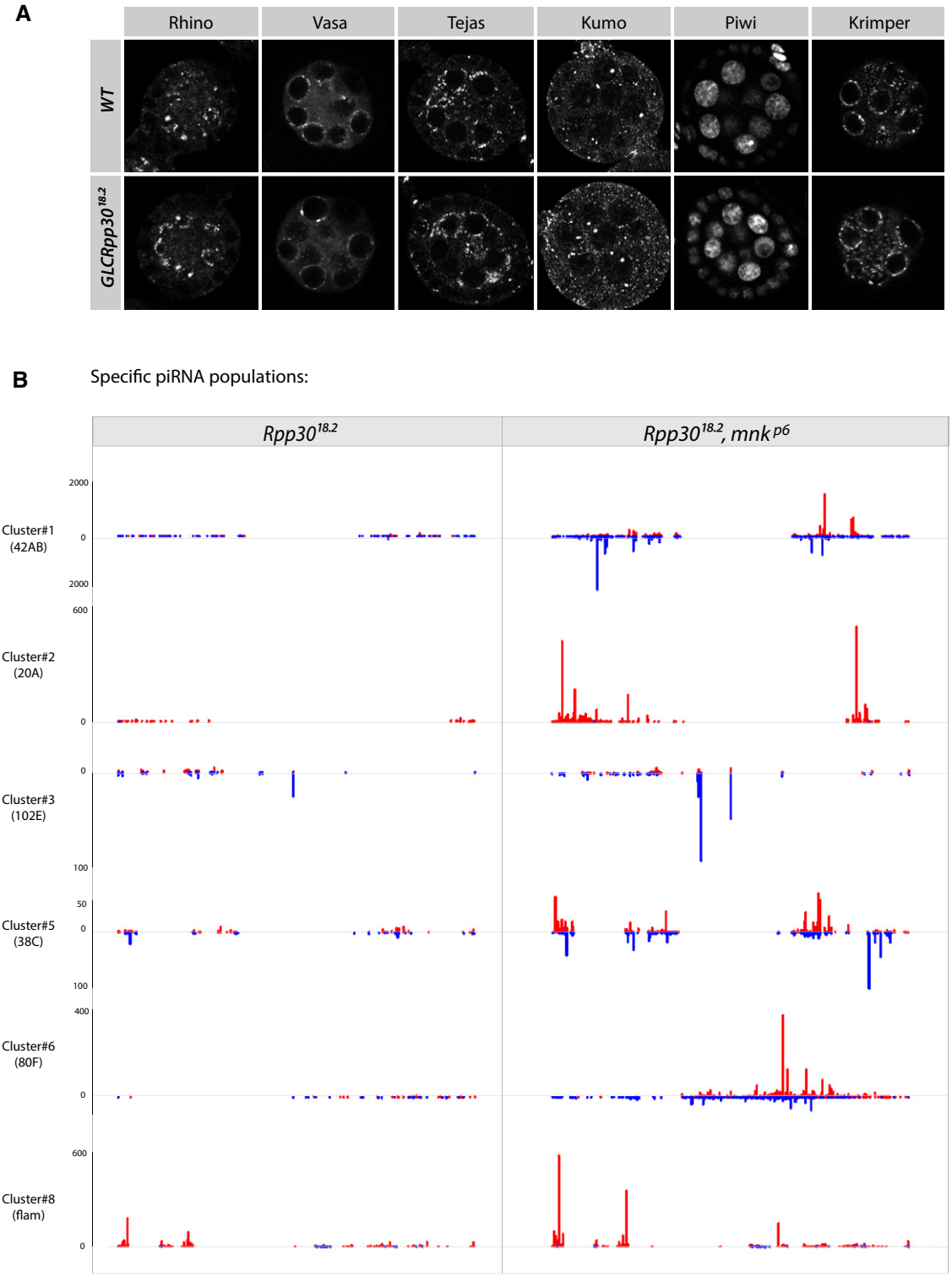

Figure EV3. piRNAs are rescued in double mutants *Rpp30, chk2* (related to Fig 5).

A Nuage-specific factors (Vasa, Tejas, Kumo, and Krimper) and Rhino and Piwi protein localizations are shown in wild-type and germ line mutant clones for *Rpp30*$^{18.2}$.

B piRNA-specific unique mappers from different piRNA clusters are shown in *Rpp30*$^{18.2}$ homozygous ovaries versus *Rpp30*$^{18.2}$, *mnk*^{p6} double-mutant ovaries. The scales are indicated on the left. Red, sense. Blue, antisense.

Source data are available online for this figure.

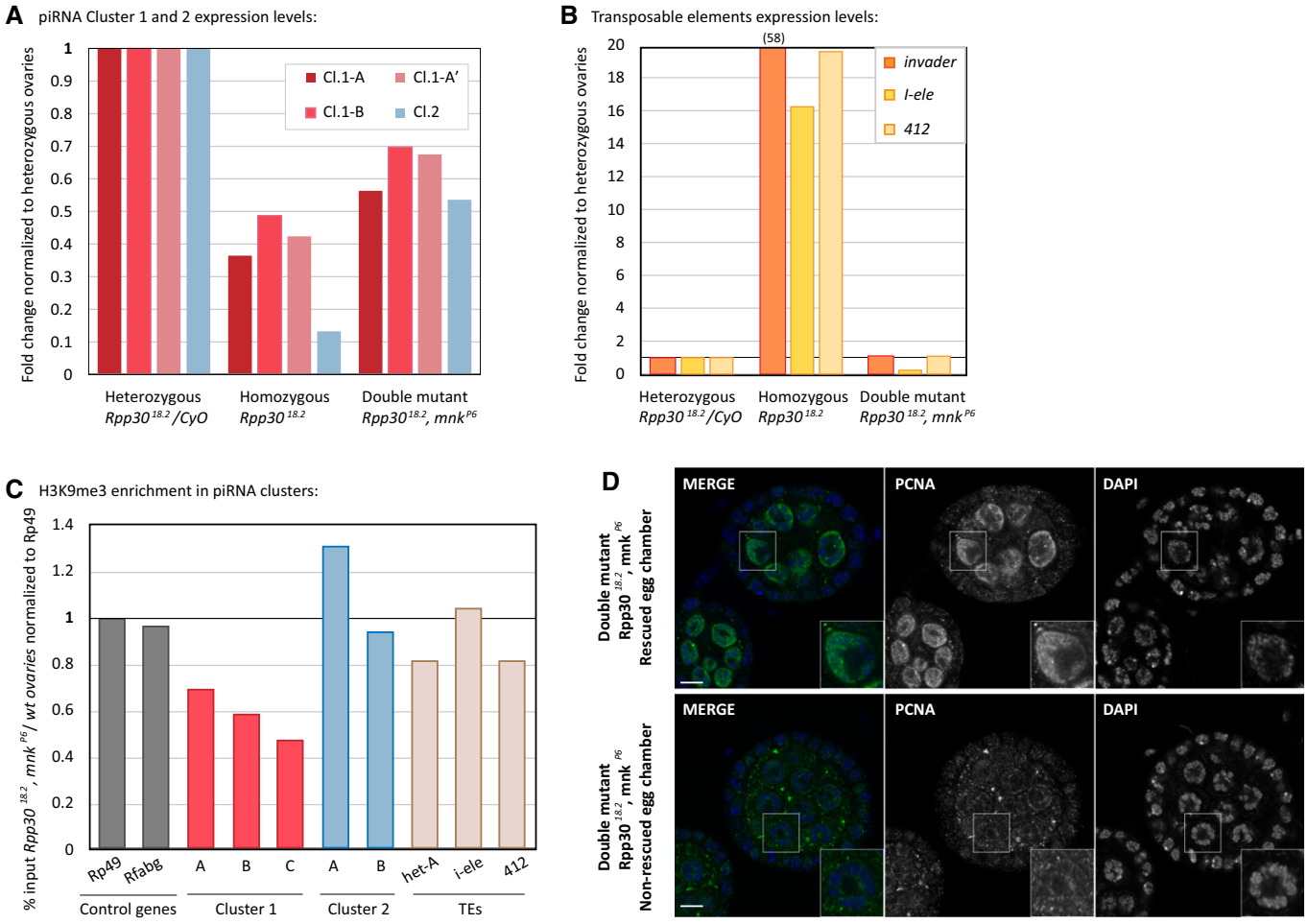

Figure EV4. *Rpp30, chk2* double mutant characterization (related to Figs 3, 4, and 6).

A, B RNA extracted from heterozygous *Rpp30*$^{18.2}$*/CyO*, homozygous *Rpp30*$^{18.2}$ and double mutant *Rpp30*$^{18.2}$,*mnk*^{p6} ovaries was used to study piRNA clusters 1 and 2 expression levels (A) and transposable element expression (B) by RT–qPCR.

C About 100 ovaries from *white* and *Rpp30*$^{18.2}$, *mnk*^{p6} were used for ChIP experiments with H3K9me3 antibody. The corrected percentage of input normalized to control genes is shown as the ratio between the double mutant and the control, reflecting a rescue of methylation profiles in different regions of the two principal piRNA clusters (1 and 2) and in some TEs (Het-A, I-ele, and 412) in double-mutant ovaries.

D Double-mutant ovaries *Rpp30*$^{18.2}$, *mnk*^{p6} were fixed and stained for PCNA. Example of one rescued and one non-rescued egg chamber are shown. Scale bar, 10 μm.

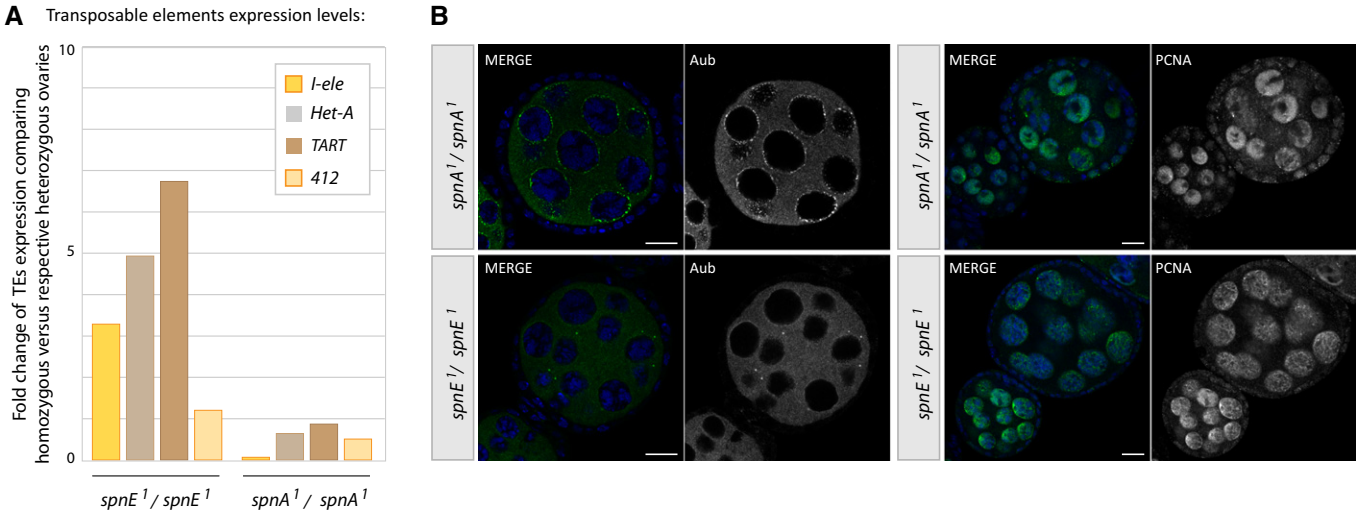

Figure EV5. Chk2 activation by *spnA* mutation does not recapitulate *Rpp30* phenotype (related to Figs 3, 5, and 6).

A RNA extracted from heterozygous or homozygous *spnA*^{1} and *spnE*^{1} flies was used to study transposable element expression by RT–qPCR. The fold change of TEs expression comparing homozygous versus respective heterozygous ovaries is shown.

B Ovaries from homozygous *spnA*^{1} and *spnE*^{1} flies were fixed and stained for Aub (left) or PCNA (right). Scale bar, 10 μm.